JOURNAL OF PROPULSION AND POWER
Vol. 21, No. 5, September–October 2005

Experimental and Model Study of Agglomeration of Burning Aluminized Propellants

Tai-Kang Liu*
Chung Shan Institute of Science and Technology, Taoyuan 325, Taiwan, Republic of China

Agglomerate sizes of ammonium perchlorate/cyclotrimethylene trinitramine/aluminum/hydroxyl–terminated polybutadiene propellants with virgin aluminum sizes of 7, 17, and 30 μm were measured by a cinephotomicrography experimental technique under 300- (2.07-) and 1000-psi(6.89-MPa) pressures. The measured sizes followed a log-normal distribution. A decrease in the virgin aluminum size leads to an increase in the mean agglomerate size. The effect diminishes when the aluminum size increases or the pressure decreases. Gany and Caveny's theory indicates that the virgin aluminum size/mobile molten layer thickness controls the degree of agglomeration. Their theory was tested and validated using data obtained from three different propellant systems. Agglomerate size data from 14 different sources in the literature were carefully reviewed. These data were obtained from aluminized composite propellants containing two different types of oxidizer: ammonium perchlorate and ammonium perchlorate and cyclic nitramines. A new agglomeration parameter λ that is a function of burning rate and propellant formulation is proposed to correlate the selected 126 agglomerate size data including 6 experimental data generated in the study. It was found that the proposed new agglomerate size model can better explain the literature data for both ammonium perchlorate/aluminum/rubber and ammonium perchlorate/nitramine/aluminum/rubber propellants rather than the Hermsen model over a wide range of experimental conditions. Validity of the new model was tested with data from a recent publication.

Nomenclature

D	=	diameter
D_{ag}	=	weight mean Al agglomerate diameter
F	=	instantaneous shooting speed
H	=	height
I_{sp}	=	specific impulse
k	=	constant in Eq. (4)
L	=	constant in Eq. (1)
L'	=	instantaneous film length
l	=	mobile molten layer thickness
N	=	number
P	=	pressure
r_b	=	burning rate
T	=	thickness
t	=	time
W	=	width or weight
λ	=	agglomeration parameter defined by Eq. (4)

Subscripts

Al	=	aluminum
i	=	individual particles
20, 40	=	under respective pressures, atm

Superscript

0	=	original

Introduction

BECAUSE of potential applications in tactical motors, the agglomeration of aluminized ammonium perchlorate (AP)/cyclotrimethylene trinitramine (RDX)/hydroxyl–terminated poly butadiene (HTPB) low-burning-rate propellants has been the subject of investigation using a quenched particles collection bomb (QPCB)[1–3] as the main experimental tool. Better understanding of agglomeration phenomena of these kinds of propellants was attempted by systematic formulation changes and quench-distance changes. Introducing RDX into the propellant matrix was found to enlarge the agglomerate size.[1,2] The adequacy of the pocket model[4] to elucidate agglomeration data for propellant containing a second oxidizer, RDX, was also tested.[3] Aluminum agglomerations have been known to degrade combustion efficiency and motor performance. It has been reported[5] that there will be approximately 1% I_{sp} loss for every 10% unburned aluminum.

A cinephotomicrography technique was developed and employed for spatially and temporally complex solid-propellant combustion studies at the U.S. Naval Weapons Center.[6] The ultra-high-speed, high-magnification movie allows slow motion viewing of combustion phenomena with minimum interference with the combustion process being studied. A cinephotomicrography experimental technique was adopted in this investigation for the condensed-phase aluminum agglomeration study. The agglomerate size and the large number of particles on a burning surface can be measured by analyzing the high-magnification still movie frames. The use of natural illumination for size determination must be treated with caution, as stated by Netzer et al.[5] and Grigor'ev et al.[7] This gave dimensions of the particle flame zone, which were larger than the true agglomerate dimension. Melcher et al.[8] and Melcher[9] recently confirmed this by using the Abel inversion technique to obtain the burning particles' true intensity profile inside a laboratory-scale solid rocket motor. Grigor'ev et al.[7] also provided an empirical formula to estimate the enlargement ratio as proportional to $P^{-0.14\sim-0.18}$, and at $P = 40$ atm, the ratio is $1.1 \sim 1.2$. From the Grigov'ev et al.[7] formula, it is clear that measurement error of the natural light high-speed camera experiments should decrease as pressure increases.

There are several motivations for this study. There appear to be some contradictions on the effects of virgin aluminum size on D_{ag} for small aluminum size ranges ($\leq$30 μm) in published works, although it is generally agreed that larger aluminum size tends to give smaller agglomerate size due to a lesser melting tendency[4] and more favorable kinetically limited leading-edge flame,[10] which will lead to much easier aluminum particle ignition. The literature survey is summarized in Table 1 and includes results from Refs. 1, 2, 5, and 10–13. Three[5,10,13] of the seven studies revealed the uncommon

Received 5 July 2004; revision received 11 March 2005; accepted for publication 18 March 2005.

*Senior Scientist, P.O. Box 90008-17-17, Chemical System Research Division, Lungtan. Senior Member AIAA.

Table 1 Comparison of experimental results for effect of aluminum size on D_{ag} or extent of agglomeration using small ($\leq$30-μm) aluminum particle size

Investigator	Al size, μm	Propellant	Results
Gany and Caveny[11]	5, 6, 12	Double base, 13%Al; $r_b = 2$–9.3 mm/s, $l = 22$–6 μm for 1.2–11.5 MPa (174–1668 psia)	1) Agglomeration is more prominent for smaller Al. 2) Experiments with 5-μm particle loadings as low as 0.1% confirmed that agglomeration occurs. 3) For Al particle diameter smaller than the mobile reaction layer thickness, prominent agglomeration takes place; for particles larger, a sharp decrease in agglomeration occurs.
Sambamurthi et al.[10]	5, 15, 30	AP/Al/PBAN, 18%Al; 0.345 and 1.38 MPa (50 and 200 psia)	1) Largest D_{ag} occurred with middle 15-μm size at both pressures. 2) Concepts of filigree formation and AP-size-related kinetically limited leading-edge flame introduced for agglomeration mechanism.
Liu et al.[1]	6, 16	AP/RDX/Al/HTPB, 16%Al, 18%RDX; 1.37, 3.45, and 6.89 MPa (200, 500, and 1000 psia)	1) Reducing Al size under 1.37, 3.45, and 6.89 MPa tends to enlarge D_{ag} from 233, 223, and 225 μm to 257, 258, and 219 μm, respectively.
Liu and Hsieh[2]	7, 17, 30	AP/RDX/Al/HTPB, 17%Al, 21.4% RDX; 2.07 and 6.89 MPa (300 and 1000 psia)	1) D_{ag} is log-normal distributed. 2) 30 μm size give smallest D_{ag} under both pressures. 3) Undistinguishable D_{ag} distribution for 7- and 17-μm size under both pressures.
Suzuki and Chiba[12]	6, 25	AP/HMX/Al/HTPB, 18%Al, 8%HMX; $r_b = 4.7$ mm/s	1) Reducing Al size enlarges D_{ag} from 197 to $(234 + 232 + 197)/3 = 221$ μm (phase III experiments).
Christian[13]	5, 25	AP/Al/HTPB, 18%Al; 1.38–11 MPa (200–1600 psia)	1) Fraction of Al agglomerates increases from 32 to 44% when Al size increases (Aerojet).
	5, 15, 20	AP/Al/HTPB, 15%Al; 1.38 MPa (200 psia)	2) Fraction of Al agglomerates decreases from 20 to 10% when Al size increases (Lockheed).
	6, 13, 23	AP/HMX/Al/HTPB, 21%Al, 17% HMX; 6.89 MPa (1000 psia)	3) Fraction of Al agglomerates decreases from 41 to 25% when Al size increases (Thiokol/Wasatch).
Netzer et al.[5]	7, 23	AP/Al/HTPB, 5%Al; 3.45 and 6.89 MPa (500 and 1000 psia); $r_b \approx 7.6$ mm/s at 500 psi, $r_b \approx 9.1$ mm/s at 1000 psi	1) Burning particle diameter increases from 150 to about 500 μm as Al size increases from 8 to 80 mm. Higher pressures lead to larger burning particle diameter.

trend of increasing agglomeration with increasing Al size. Churchill et al.[14] conclude that aluminum particle size is not a significant factor at low burning rates for controlling D_{ag}. King[15] claims that there would be no agglomeration when virgin mass median Al particle size exceeds 50 μm. The definition of agglomerate size was given by Sambamurthi et al.,[10] who took condensed combustion products as agglomerates when the average size exceeds 49 μm, and recently by Glotov et al.[16] and Glotov and Zarko[17,18] for particles with diameter larger than 60 μm. These criteria were used to screen the literature data for the agglomerate size modeling study in this paper.

This investigation attempted to correlate the reported D_{ag} data in the open literature within the virgin aluminum size range ($\leq$50 μm) with model parameters consisting of propellant formulation variables and burning rate. Both AP/Al/HTPB and AP/Al/cyclic nitramine/HTPB propellants were considered. Hermsen's model[19] is perhaps the most widely used engineering model for estimation of D_{ag} of AP/Al/rubber propellants. However, it has been noted that this model does not consider the effect of aluminum concentration.[20] Besides, the accuracy of Hermsen's model for predicting D_{ag} in low-AP-content and low-burning-rate region appears doubtful.[2] Duterque[20] has provided a review of the Al agglomerate size prediction model. In addition to four correlation models surveyed by Duterque,[20] Kovalev[21] has recently proposed an elaborate agglomerate size prediction model based on solving agglomerate mass and energy dynamic conservation equations.

The burning rate is a dominant factor that affects D_{ag}; the latter is inversely proportional to burning rate in the Hermsen prediction model.[19] In this investigation, we have incidentally formulated an AP/RDX/Al/HTPB composite propellant with burning rate [3.25 mm/s at 2.07 MPa (300 psia) and 6.3 mm/s at 6.89 MPa (1000 psia)] very close to Gany and Caveny's aluminized double-base propellant[11] [3 mm/s at 2.07 MPa (300 psia) and 6.5 mm/s at 6.89 MPa (1000 psia), Fig. 3 of Ref. 11]. The mobile reaction-layer thickness in Gany and Caveny's study, which decreases with increasing pressure, is between 6 and 14 μm in the earlier cited pressure range (Fig. 3 of Ref. 11). The reaction-layer thickness is thinner compared with our previous AP/RDX/Al/HTPB propellant study[1] which shows that the combustion wave can affect the condensed phase down to approximately 100 μm beneath the burning surface due to RDX melting. (Figure 10 of Ref. 1 shows that bubbles due to decomposition reacting gases products entrapped within the melt are observed down to an approximate 100 μm depth from a side-cut micrograph obtained from rapid-depressurization experiments.) Based on Gany and Caveny's theory[11] that the relative dimensions between Al size and reaction-layer thickness can dominate the degree of agglomeration, it would be interesting to compare these two kinds of propellants with such a wide mobile-layer thickness difference but very close burning rates. Melcher's study[9] reported a large number of surface diameter data between 5.9 and 21.2 atm (0.6 and 2.15 MPa) for agglomerating propellant (Alliant 1). From the reported propellant burning rate equation, pressure, propellant thermal diffusivity, virgin Al size, and agglomerate sizes, it is also possible to test Gany and Caveny's agglomeration theory using Melcher's experimental data.

In summary, the objectives of this investigation are 1) to measure experimentally the aluminum agglomerate size of AP/RDX/Al/HTPB propellants on a burning surface with virgin aluminum size and pressure changes by use of a cinephotomicrography technique and 2) to model the aluminum agglomerate size on a burning surface using literature data and experimental results from this study for composite propellants with oxidizers containing either AP only or AP/cyclic nitramine mixture.

Experimental

Propellants

Three AP/RDX/Al/HTPB propellants with the same composition but different Al sizes were prepared using a Baker Perkins laboratory blender. Ingredients percentages in weight are AP (400 μm) 25%, AP (225 μm) 25%, RDX (110 μm) 21%, Al (average diameters 7, 17, and 30 μm with trade names H5, H15, and H30,

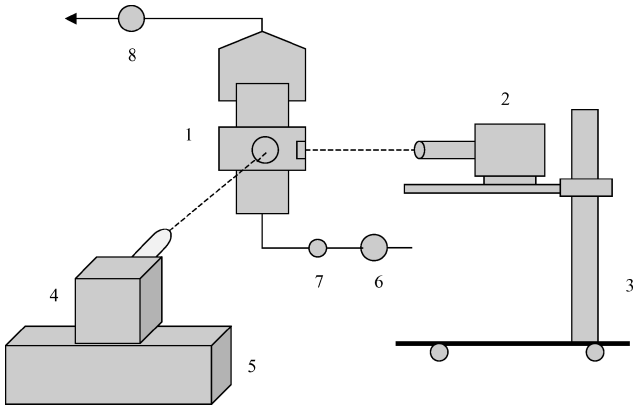

Fig. 1 Experimental setup schematic: 1) windowed bomb, 2) PHOTEC-IV high-speed camera, 3) camera stand, 4) 1000-W Xe arc lamp, 5) 1000-W power supply, 6) pressure regulator, 7) pressurization gas inlet valve, and 8) purge gas flow adjusting valve.

respectively) 17%, and HTPB 12%. All dimensions reported were volume-averaged as measured by the Malvern Mastersizer 2000. The propellants were burned at two pressures, 2.07 and 6.89 MPa (300 and 1000 psig), under flowing nitrogen. The strand burner burning rates were 3.25 and 6.3 mm/s under respective pressures. The effect of Al size on the burning rate was negligible. The aluminum particles were spherical in shape.

Windowed Bomb and Sample Preparation

A stainless steel high-pressure device similar to that used in Ref. 6 with 320-ml (3.2×10^{-4} m^3) internal volume was constructed with two thick, fused quartz viewing windows at about 60 deg apart. A small window is used for sample viewing and photography whereas a large window is used for the external illuminating light source. The propellant sample 12 mm high by 10 mm wide by 3 mm thick was bevel cut 45–60 deg on the $H \times T$ plane. The sample was installed in the bomb with the inclined plane facing the high-speed camera. The bomb was pressurized with flowing nitrogen. A hot-wire igniter and a small amount of B/$BaCrO_4$/NC/acetone fast-burning mixture on top of propellant sample were used to ensure uniform ignition. The schematic of experimental setup is shown in Fig. 1.

High-Speed Camera

Model Photec-IV made by Photonic System, Inc., was used. The rated speed ranged from 100 to 10,000 frames/s (FPS) with a doubling speed and one-half frame if a half frame converter is installed. The camera resolution is 68 lines/mm, or about 15 μm. Eastman color 16-mm high-speed negative film was used (Model 7251, 7296) with a length of 30.5 or 122 m (100 or 400 ft) made by Kodak Company. The shooting speed was fixed at 4000 and 8000 FPS under 2.07 and 6.89 MPa (300 and 1000 psia), respectively.

Lenses

A Mamiya-M645 150-mm lens coupled with five autoextension rings (numbers 1×1, 2×2, and 3-S $\times$ 2) and 80 A filter were used. The f/stop setting was 22–32, which gives a better depth of field for a bevel cut inclined sample surface. The field of view was about 9 mm high by 11 mm wide. The duration of combustion process recorded by the camera, depending on propellant burning rates and pressure, can be varied between 0.3 and 1.4 s.

Illuminator

Lamp housing, Model LH-153, was made by Spectral Energy Company. Inside the lamp housing was a 1000 W xenon arc lamp model XM1000-21 made by Optical Radiation Company. A secondary focusing lens, Model LHA-150/3, was installed near the outlet of the arc lamp for further light focusing. The power supply, rated 1000 W and 45 A, was made by Kratos Company, Model LPS-255HR. To prevent the premature ignition of the propellant sample due to strong light energy, a movable stainless steel mechanical gate was installed opposite to the external illuminating light source window to block the strong incident light while under system standby condition. Operation of the gate was conducted by a sequential control loop.

Photographic Operation Control

A great deal coordination among different hardwire and operation procedures was required to obtain good-quality films for detailed image analysis under the desired shooting speed. Photographic operation control was conducted in a centralized panel by a sequential control loop, which controls the system power, ignition power, lifting of the mechanical gate while on standby, and triggering the high-speed camera operation. Digital timers used included test cycle timer (5 s), ignition delay timer (1.2–1.45 s), and camera-start delay timer (0.2 s).

Motion Film Analysis

The developed films were analyzed with a film motion analyzer model PH-160F made by NAC Incorporated of Japan. Generally the film can be magnified 25 times with a resolution of less than 20 μm. Accurate times of magnification can be obtained from sample image width as measured on the NAC film motion analyzer screen divided by actual sample width. The analyzer allowed for a still photograph of a selected frame. To determine the instantaneous shooting speed of a frame, F, or the speed under a specified film length L', an exponential form correlation was employed for conversion:

$$F(t) = \text{FPS}_{\text{setting}} \times [1 - \exp(-L'(t)/L)] \tag{1}$$

For speed setting of 4000 and 8000 FPS, $L = 17.54$ and 65.7, respectively, if both L' and L are in feet dimension. The predicted F deviates from actual F calculated from red dot timing marks generated in film by less than 3.5%. Figure 2 shows the comparisons for a 30.5-m (100-ft) film with speed setting of 4000 FPS. L' in Eq. (1) can be further converted to count number (CN) read by the film motion analyzer from a linear relationship between CN and L', thus gaining more convenience to obtain the speed for any specific frame,

$$L' = \text{CN} \times 7.62/(12 \times 25.4) \tag{2}$$

Where 7.62 is the nearby frame pinhole distance of the 16-mm film in millimeters and 12 and 25.4 are length conversion factors.

Surface Agglomerate Size Measurements and Data Reductions

To obtain agglomerate size on burning surface with a representative distribution, we measured agglomerate size from many

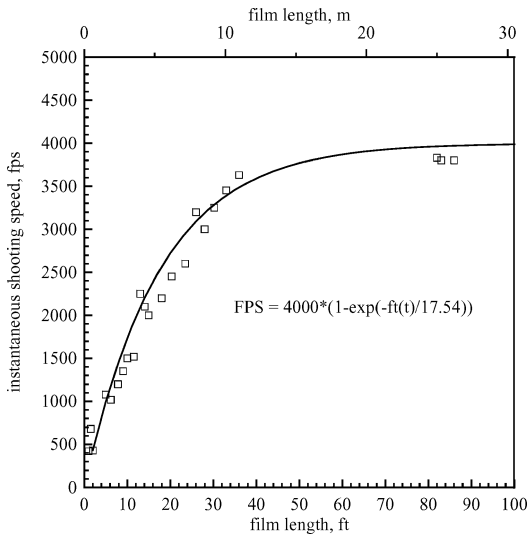

Fig. 2 Shooting speed dependence on film length (speed setting 4000 FPS).

frames when the film speed exceeded 3000 FPS (for 30.5-m film) or 7000 FPS (for 122-m film) without any repeat measurements until the total number of agglomerates counted was from near 700 to near 2500 for each of the six experimental conditions (three different aluminum size propellants each under two pressures). A previous similar study[20] using a high-speed camera only counted 50–80 particles for each test. Grigor'ev et al.[7] used not less than 600 particles to construct the cumulative particle size distribution. Thus, a high degree of confidence on the size distribution data has been ensured. The individual measurements are then sorted by Microsoft Excel spreadsheet with an interval size range of 10 μm. D_{ag} is calculated by

$$D_{ag} = (\Sigma W_i D_i)/(\Sigma W_i) = \left(\Sigma N_i D_i^4\right)\Big/\left(\Sigma N_i D_i^3\right) = D_{43} \qquad (3)$$

Results and Discussion

Agglomerate sizes of AP/RDX/Al/HTPB Propellants

Figure 3 shows the typical burning surface phenomena of the three propellants with different Al sizes under two pressures. The bright droplets are Al agglomerates. The dark zone beneath the agglomerates is unburned solid propellant. For the same Al size, larger agglomerates are observed under low pressures. The contrast becomes more obvious when Al size becomes larger. For the same pressure, smaller effects of Al size on agglomeration are observed under lower pressures. However, larger differences are found due to the Al size effect under higher pressure, that is, the extent of agglomeration become smaller as Al sizes become larger, although the difference diminishes as Al size become larger. More smoke trails are observed for low-pressure pictures due to higher nitrogen mass flow rates used under low pressure. The trailing phenomena of burning Al in a mild convective flow had been observed by Price.[22,23]

Figures 4 and 5 show the cumulative weight percentage of agglomerate diameter under different pressures. Each symbol in Figs. 4 and 5 represents from 1 to near 400 counts. Nearly straight lines are observed in both Figs. 4 and 5, indicating the log-normal distributions. The same kind of distribution can be found from our previous study[2] using a similar kind of propellant by use of a nonoptical

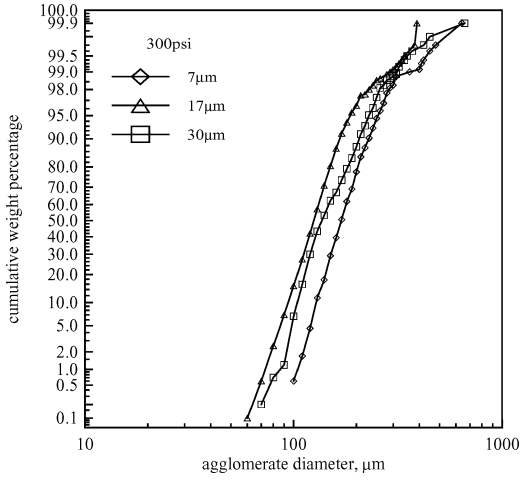

Fig. 4 Cumulative weight percentage of agglomerate diameter as function of virgin aluminum size under 300 psi (2.07 MPa).

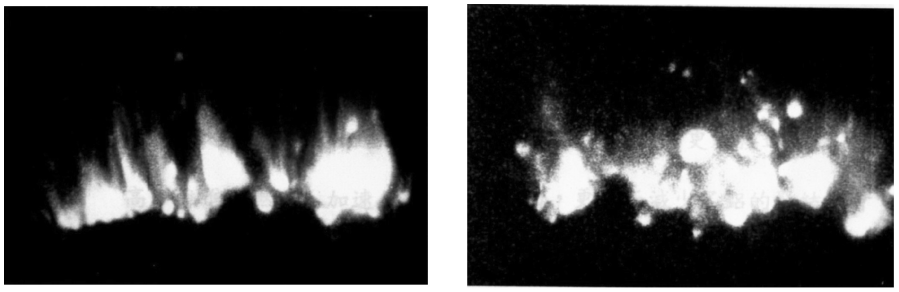

a) 7 μm

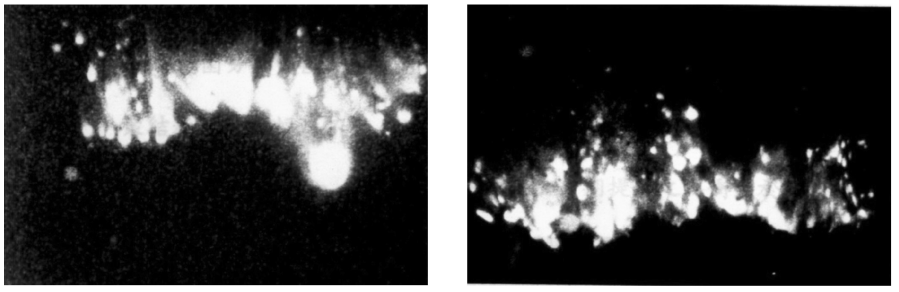

b) 17 μm

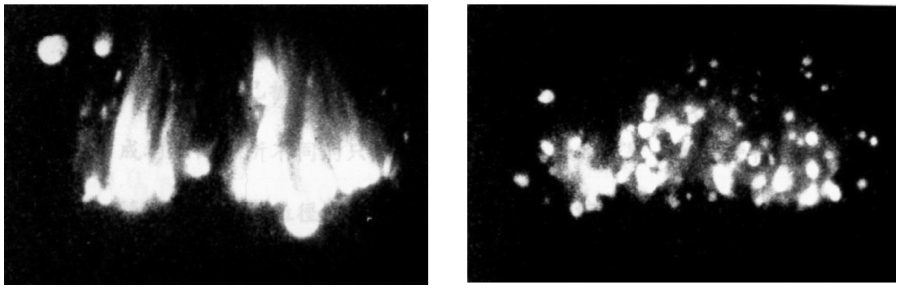

c) 30 μm

Fig. 3 Typical burning phenomena at or near burning surface for propellants with the same composition but different virgin aluminum sizes and pressures; left, 300 psi (2.07 MPa) and right, 1000 psi (6.89 MPa).

Table 2 D_{ag} obtained under various conditions

Pressure, psi (MPa)	Al size, μm	Agglomerate size range, μm	Number of agglomerates counted, high-speed film	D_{ag}, μm
300 (2.07)	7	100–760	691	287
300 (2.07)	17	60–810	991	275
300 (2.07)	30	70–720	1008	264
1000 (6.89)	7	110–350	1566	225
1000 (6.89)	17	40–410	1804	176
1000 (6.89)	30	50–350	2448	162

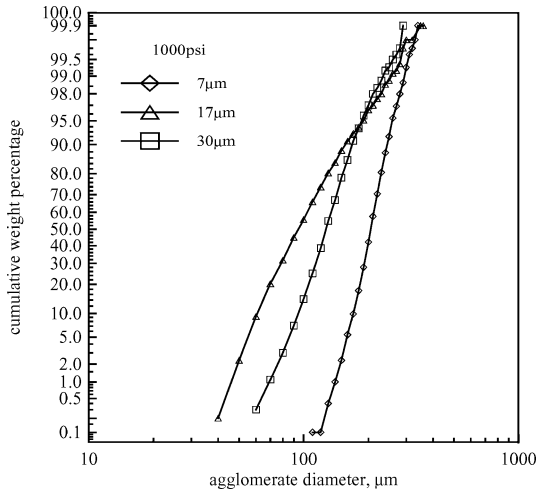

Fig. 5 Cumulative weight percentage of agglomerate diameter as function of virgin aluminum size under 1000 psi (6.89 MPa).

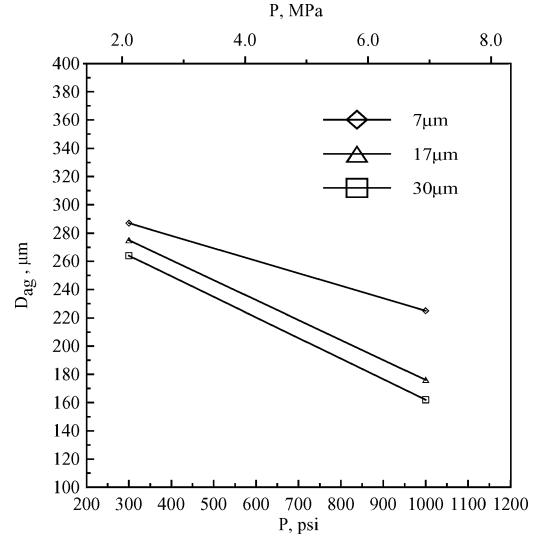

Fig. 6 Dependency of D_{ag} with virgin aluminum size and pressure.

experimental method (QPCB) and the Grigor'ev et al. study[7] using low-oxidizer content AP/Al/rubber propellants with an optical method. Both Fig. 4 and the left side of Fig. 3 show the almost indistinguishable large agglomerate size under low pressure. Both Fig. 5 and the right side of Fig. 3 show the distinct large agglomerate size for 7-μm Al under high pressure. Table 2 summarizes the experimental results of Figs. 4 and 5.

Figure 6 shows the dependency of D_{ag} with the virgin Al size and the pressure listed in Table 2. Decreasing D_{ag} is shown as pressure increases. The smallest Al size gives the largest D_{ag}, especially under high pressure. Although Fig. 6 reveals the overall trend of increasing D_{ag} as Al size decreases, the effect diminishes when Al size increases or pressure decreases. The latter observation is in agreement with that of Churchill et al.[14] from QPCB experiments that aluminum particle size is not a significant factor for controlling D_{ag} at low burning rates.

AP/RDX/Al/rubber propellants containing a substantial amount of the second oxidizer RDX, which melts around 480 K (207°C), which is lower than typical propellant surface temperature of ~900 K (Ref. 22), will probably demonstrate a different agglomeration scenario when compared with AP/Al/rubber propellants and aluminized double-base propellants. AP particles that are 400 and 225 μm average size in the formulations of this study have no appreciable size effect on condensed-phase agglomeration, which was noted in our previous study[3] using AP/RDX/Al/HTPB propellants. Based on our previous study,[3] there were almost no agglomerate size distribution changes (CB06 vs CB16) even though the proportion of 400 and 225 μm AP varies between 90/10 and 60/40. The AP particle heating process involves a series of steps, such as phase change from orthorhombic to cubic, formation of a liquid surface, liberation of gases, chemical reactions, etc. It has recently been determined[8,9] that the condensed-phase liquid layer thickness is about 5 μm (Ref. 6) or about 14–36 μm under the respective pressures of 13.4–1 atm (1.36–0.1 MPa) as determined recently.[8,9] RDX crystals, with average diameter of 110 μm used in this investigation, are about two-fifths that of AP particles by weight and from about one-half to one-quarter that of AP particles by diameter. Thus, that the smaller RDX crystals disperse within coarser AP particles can be postulated. The fine Al particles, with average diameter of 7, 17, or 30 μm used in this investigation, are concentrated in the pocket formed by these two kinds of oxidizers. Inside the oxidizers' space are also bridges formed by binder and virgin aluminum particles. Al particles can form molten pools as they reach the burning surface, which agglomerate into larger droplets, or, alternatively, form large droplets through sinter and/or coalesce mechanisms. The RDX crystals melt and mix with the binder melt layer and aluminum particles/agglomerates before burning to present a planar surface. Because of the melting process of RDX crystals, the combustion waves can affect the condensed phase down to approximately 100 μm beneath the burning surface.[1] This distance is much larger than the 5–36 μm liquid layer thickness of AP particles.[6,8,9] Therefore two kinds of Al burning and agglomeration processes may simultaneously occur as combustion wave propagates. The Al particles residing away from RDX particles are affected by a thin AP liquid layer, AP monopropellant flame, and intensive primary diffusion flame from the decomposition products of AP and the rubber binder. An agglomerate, if formed on the surface or in the pocket, may ignite as it emerges next to an AP/rubber flamelet where oxidizing species are available for ignition. However, Al particles in a close vicinity to RDX particles are hindered by both the retention of a thick RDX melt layer and a lesser oxidizing monopropellant flame and diffusion flame due to fewer oxidizing fragments in the RDX molecule structure than AP, leading to less favorable Al ignition and resulting in a larger agglomerate than Al particles away from RDX. This postulated scenario is in agreement with that of Babuk,[24,25] who cited the Russian agglomeration studies that the formation of oxidizer in melted state increases the mass-medium diameter of agglomerates by 2–3 times. The scenario is also in agreement with the literature experimental data, in which larger agglomeration zone are mostly associated with propellants containing RDX or HMX, as will be shown later. Thus, the agglomeration process of AP/RDX/Al/rubber propellant is possibly localized due to RDX. The larger D_{ag} shown in Figs. 4 and 5 could have a greater chance of resulting from Al particles residing near RDX crystals than AP particles. This heterogeneous scenario may be evident from the observed localized large bright agglomerate particles shown in Fig. 3.

Gany and Caveny[11] studied the Al agglomeration of aluminized double-base propellants. The virgin Al size of our study is within zone 2 (smaller size) and zone 3 (larger size) of their study, in which agglomeration and minimum agglomeration can be expected, respectively (Fig. 5 of Ref. 11). Because of the homogeneous nature of double-base propellants, the microstructure and combustion characteristics of their propellant should be different from the one described earlier here. When the near-equal burning rates between

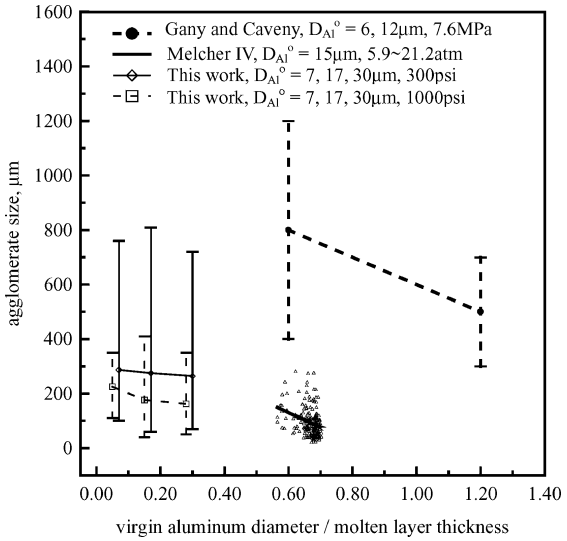

Fig. 7 Effect of D_{Al}^{0}/l on agglomerate size.

our AP/RDX/Al/HTPB propellant and their aluminized double-base propellant is considered, an equal chance of Al particles ignition due to equal time exposure to the gas-phase flame can be roughly expected. The molten-layer thickness, however, is widely different in each study. Gany and Caveny[11] proposed that the relative dimensions between virgin Al size and reaction-layer thickness can dominate the degree of agglomeration, that is, the smaller the value of D_{Al}^{0}/l, the larger the tendency for Al agglomeration. Figure 7 shows the dependency of agglomerate size on D_{Al}^{0}/l for both studies. The agglomerate size limits of our study and of Gany and Caveny were taken from Table 2 and the size estimation from Figs. 6a and 6b (at 7.6 MPa) of Ref. 11, respectively. The molten-layer thickness of our study and that of Gany and Caveny were taken as 100 μm (Ref. 1) and 10 μm (at 7.6 MPa in Fig. 3 of Ref. 11), respectively. Figure 7 shows that rough similarities are observed among individual D_{Al}^{0}/l ranges, thus, tentatively validating their agglomeration theory. Furthermore, Melcher's study[9] reported 194 surface agglomerate size data for the pressure range between 5.9 (0.6) and 21.2 atm (2.15 MPa) (Ref. 9, Table B.2, pp. 212–216). Melcher[9] used agglomerating propellant (Alliant 1) loaded with 15-μm Al. The propellant burning rate equation is $r_b = 0.17P^{0.37}$ and the thermal diffusivity is 6.1×10^{-4} cm^2/s (6.1×10^{-8} m^2/s). Molten-layer thickness can be calculated from thermal diffusivity/burning rate. Figure 7 shows that, like the other two cases, a negative slope (−544.77) can be obtained from the linear least-square fitting of the 194 data, further illustrating the adequacy of Gany and Caveny's theory. It appears, however, that more effort is needed to implement this mechanistic result to agglomerate size prediction.

Agglomerate Size Modeling of Aluminized Composite Propellants

A new agglomeration parameter, λ, is used to correlate the average agglomerate size experimental data from the open literature and this study for aluminized composite propellants. In certain cases, the acquisition of the literature data was not straightforward because the reported experimental data were not always accompanied by all of the required parameters shown in Eq. (4). Only those works having parameters shown in Eq. (4) will be used in this modeling. Thus, $D_{ag} = k\lambda$ where

$$\lambda = (\text{wt\% of Al} + \text{wt\% of cyclic nitramine} + 1)\Big/ \Big\{[\text{wt\% of AP} + \text{wt\% of cyclic nitramine}] \times r_b(\text{mm/s}) \times \left[D_{Al}^{0}(\mu\text{m})\Big/50 + 1\right]\Big\} \quad (4)$$

Increasing the values in the numerator of Eq. (4) increases agglomeration, as supported from our experience that both Al and nitramine increase the agglomeration tendency. Increasing the values of the denominator in Eq. (4) decreases agglomeration, from the understanding that the AP diffusion flamelet facilitates Al ignition more than agglomeration and that high burning rate decreases Al residence time on the burning surface, thus decreases the chance for sintering and agglomeration. The last term in the parentheses of the denominator is to take into account the effect of virgin aluminum size on agglomeration. In Eq. (4), 50 is taken from King,[15] who maintained that there will be no agglomeration when the virgin aluminum size is greater than 50 μm. In Eq. (4), 1 in both the numerator and denominator is for the purpose of reducing our model to the Hermsen model when the three new parameters in Eq. (4), namely, wt% of Al, wt% of cyclic nitramine, and D_{Al}^{0} are set to zero. The Hermsen model[19] is given as

$$D_{ag} = 35(\mu\text{m})/[\text{AP mass fraction} \times \text{burning rate (in./s)}] \quad (5)$$

The effect of both kinds of oxidizers on agglomeration can be considered in Eq. (4) instead of Eq. (5). Agglomeration parameter λ for propellants without the second oxidizer, that is, cyclic nitramines, can be calculated when the weight percentage of nitramine in Eq. (4) is equal to zero. When Eq. (4) is used, it is assumed that both RDX and HMX are exhibiting the same role when exerting their effects on Al agglomeration.

Summaries in the literature of agglomerate size experiments for AP aluminized composite propellants either containing cyclic nitramine or not are shown in Tables 3 and 4, respectively. For the total of 14 sources, the number of sources containing cyclic nitramines (five cases) is less than the one without nitramines (nine cases). These data were from experiments covering a wide range of formulations, pressures, burning rates, experimental facilities, and agglomerate sizes. With the exception of works of Grigor'ev et al.,[7] Christian,[13] Churchill et al.,[14] and Glotov and Zarko,[17] almost all of data from other studies were used for this modeling. The data screening criteria for Refs. 7, 13, 14, and 17 are detailed in the footnotes of Tables 3 and 4. A total of 126 agglomeration experimental data including six from the experimental part of this paper were obtained and calculated with a Microsoft Excel spreadsheet. The data are first compared with the Hermsen model, as shown in Eq. (5), then with our new model, shown in Eq. (4).

Figure 8 shows that, with the exception of the three data groups from Glotov and Zarko,[17] Babuk,[24,25] and Murai et al.,[26] out of a total of nine data groups from the no-nitramine category shown in Table 4, the Hermsen model overpredicts D_{ag} for aluminized propellants. Furthermore, Fig. 9 shows that all five cases from the with-nitramine groups (Table 3) are also overpredicted by the Hermsen model. Overprediction of with-nitramine data is possibly due to a smaller value being used in the denominator of Eq. (5) wherein

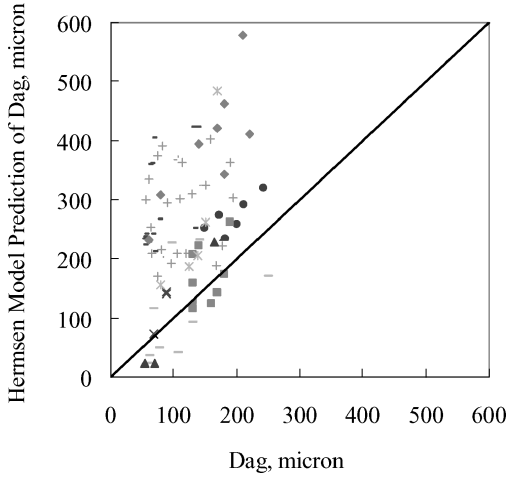

Fig. 8 Comparison of agglomerate sizes between experiments and Hermsen model predictions for AP/Al/rubber propellants: ●, no nitramine, Suzuki and Chiba[12]; +, no nitramine, Christian Figs. 5–9[13]; -, no nitramine, Churchill et al.[14]; —, no nitramine, Babuk[24,25]; ♦, no nitramine, Grigor'ev et al.[7]; ■, no nitramine, Murai et al.[26]; ▲, no nitramine, Glotov and Zarko[17,18]; × , no nitramine, Kraeutle et al.[27]; and ✳, no nitramine, Duterque.[20]

Table 3 Agglomerate size studies for aluminized composite propellants containing cyclic nitramine and AP

Reference	Propellant	Experimental				
		Pressure, MPa	r_b, mm/s	Facility	D_{ag}, μm	Data points
This work	AP: 50%, RDX: 21%, RDX size: 110 μm, Al: 17%, Al size: 7–30 μm, HTPB: 12%	2.07–6.89	3.85–6.26	High-speed cinephotomicrography	162–287	6
Liu and Hsieh[2]	AP: 49.6%, RDX: 21.4%, RDX size: 110 μm, Al: 17%, Al size: 7 μm, HTPB: 12%	2.07–6.89	3.86–6.25	QPCB	210–375[a]	2
Suzuki and Chiba[12]	AP: 54–64.8%, HMX: 7.4–15%, HMX size: 20–200 μm, Al: 15.7–20%, Al size: 6–25 μm, HTPB: 10.4–12%	2.03	4.16–5.53	Combustion photograph	152–343	23
Christian[13] (Figs. 11 and 12)	AP: 49–59%, HMX: 10–20%, HMX size: 6–90 μm, Al: 20%, 30 μm, HTPB: 11%	3.45	5.6–6.1	QPCB	75–152[b]	6[c]
Glotov and Zarko[17,18]	AP: 27–44.9%, HMX: 23.3–35%, HMX size: 160–1000 μm, Al: 16.8–22%, Al size: 6–14 μm, binder: 14.9–20%	0.6–6.4	3.6–63	Flow through bomb	50–270	6[d]

[a]Steady value of Fig. 3.
[b]Calculated from King's correlation[15] for predicting D_{ag} from the given fractional agglomerated data.
[c]Thiokol/Wasatch data were eliminated due to no burning rate data, leaving a total of eight points in Figs. 11 and 12. Two points excluded based on the criterion that there is no agglomeration when fractional agglomerated $\leqq$0.15, which gives $D_{ag} \leqq 50$ μm.
[d]Propellant identified as I1, EM1, Y1, and Y4. Propellants with aluminum powder prepared by electro-explosion of aluminum wire (Alex) were not included due to possibly different agglomeration mechanisms as compared with other propellants.

Table 4 Agglomerate size studies for aluminized composite propellants containing AP as the only oxidizer

Reference	Propellant	Experimental				
		Pressure, MPa	r_b, mm/s	Facility	D_{ag}, μm	Data points
Suzuki and Chiba[12]	AP: 68–71%, Al: 18%, Al size: 6–35 μm, HTPB: 11–14%	2.03	4.09–5.52	Combustion photograph	149–242	7
Christian[13] (Figs. 5–9)	AP: 67–72%, Al: 15–20%, Al size: 5–30 μm, HTPB: 11–18%	1.38–3.45	3.3–7.3	QPCB	56–195[a]	25[b]
Churchill et al.[14]	AP: 65–73.2%, Al: 10–20%, Al size: 5–40 μm, HTPB: 15–18.4%	1.38–4.14	3–5.74	QPCB	50.7–136.1	14[c]
Babuk[24,25]	AP: 64%, Al: 24%, Al size: 4 fractions with diameter up to 50 μm, isoprene rubber: 12%	1–6	5.9–58.4	Constant volume bomb	59–250	9[d]
Grigor'ev et al.[7]	AP: 48%, Al: 21%, Al size: 20μm, binder: 31%	2.03–4.05	4–8	Direct–shadow motion picture microphotography	60–220	8[e]
Murai et al.[26]	AP: 68–70%, Al: 18–20%, Al size: 30 μm, HTPB: 12–14%	3–7	5–11	Quench bomb method	130–190	9[f]
Glotov and Zarko[17,18]	AP: 61.8–65%, Al: 20–23%, Al size: 6–14 μm, binder: 15–15.2%	4.1–4.4	6–63	Flow through bomb	55–165	3[g]
Kraeutle et al.[27]	AP: 62.5–67.5%, Al: 17.5%, Al size: 7 μm, binder (CTPB or carboxyl-terminated polybutadiene, or TPE or trifunctional polypropylene glycol capped with ethylene oxide, or PEG or polyethylene glycol): 15%	2.16	9–18	Window bomb	68–88	3[h]
Duterque[20]	AP: 68%, Al: 18%, Al size: 15–30 μm, binder: 12%	0.2–4	2.7–8.4	High speed camera	80–170	5

[a]Calculated from King's correlation[15] for predicting D_{ag} from the given fractional agglomerated data.
[b]Total of 47 points in Figs. 5–9: 22 points excluded based on following criteria: 1) no agglomeration occurs when fractional agglomerated $\leqq$0.15, which gives $D_{ag} \leqq 50$ μm, 7 points; 2) erratic data when fractional agglomerated $\geqq$0.63, 4 points; 3) unbalanced composition of Lockheed data in Fig. 7, 2 points; 4) no burning rate data of Figs. 8 and 9, 6 points; and 5) controversial data from Aerojet in Fig. 9, 3 points.
[c]Data eliminated for this analysis as follows: 1) $D_{ag} \leqq 50$ μm, 2) CTPB binder, and 3) treated aluminum.
[d]Obvious outliner of 504 μm in Table 2.2 not used; virgin D_{Al} was obtained by weight average of median Al fraction size of each fraction.
[e]Data from Table 1 and burning rate of Fig. 5 used; composition 1 data excluded due to $D_{ag} \leqq 50$ μm; compositions 8–12 data excluded due to too high Al content (29–41 wt%) and too low AP content (37–45 wt.%), thus have no practical applications. Original volume fraction data of Al and AP were converted to weight fraction using the specific gravities of AP, 1.95; Al, 2.7; and binder, 0.92.
[f]Data taken from Ref. 28 and Figs. 6 and 7; mean Al mass diameter of 30 μm of BP-204J taken from Khono, M. *Proceedings of the 19th International Symposium on Space Technology and Science*, 1994, pp. 117–128. BP-201J and BP-203J assumed to have the same Al diameter as BP-204J.
[g]Propellant identified as EM2, EM3, and H1. Propellants with Alex were not included due to possibly different agglomeration mechanisms as compared with other propellants. Propellant 12 was not considered due to large variation of D_{ag} in a narrow burning rate range.
[h]Linear corrections performed (multiply by 2.5/2.16) for reported burning rate to estimate real burning rate.

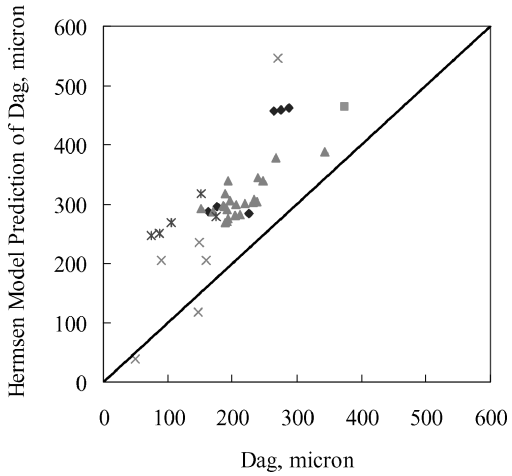

Fig. 9 Comparison of agglomerate sizes between experiments and Hermsen model predictions for AP/Al/nitramine/rubber propellants: ♦, with RDX, this work; ■, with RDX, Liu and Hsieh[2]; ▲, with HMX, Suzuki and Chiba[12]; ✳, with HMX, Christian Figs. 11 and 12[13]; and ×, with HMX, Glotov and Zarko.[17,18]

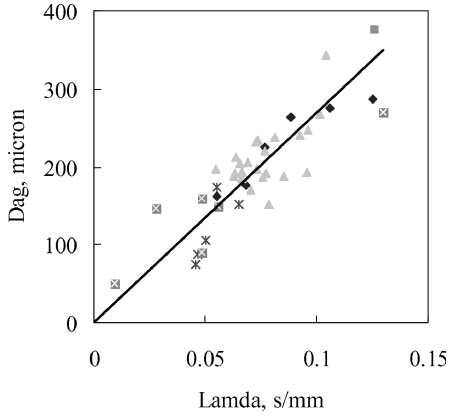

Fig. 10 Dependency of agglomerate size on lamda for AP/Al/nitramine/rubber propellants: ♦, with RDX, this work; ■, with RDX, Liu and Hsieh[2]; ▲, with HMX, Suzuki and Chiba[12]; ✳, with HMX, Christian Figs. 11 and 12[13]; and ⊠, with HMX, Glotov and Zarko.[17,18]

nitramine oxidizer content has not been taken into account in the AP mass fraction term. Besides, the Hermsen model ignores important parameters such as Al mass fraction and particle size which also contribute to prediction inaccuracy.

Figure 10 shows the dependency of λ with D_{ag} (from Table 3) for AP/nitramine/Al/HTPB propellants. Figure 10 shows a better prediction than the Hermsen model (Fig. 9) with the same experimental data. The correlation model is given by

$$D_{ag} = 2686\ (\mu\text{m})\lambda \tag{6}$$

with $R^2 = 0.74$. R^2 is the coefficient of multiple determination, a statistic for measuring the proportion of total variation about the mean response explained by the regression equation. It has a value between 0 and 1. The larger the value, the better the fitted equation explains the variation in the data. Notice in Fig. 10 that the six experimental data points from this work are apart from each other over a quite large λ range due to different virgin aluminum size and burning rate, illustrating the adequacy of parameter λ to take into account these effects. Moreover, adequacy of the model can be further validated from Glotov and Zarko's six experimental data[17] covering an even wider λ range due to a wide formulation range and an even wider burning rates range (3.6–63 mm/s).

Adding the D_{ag} data from no-nitramine aluminized propellants shown in Fig. 8 (Table 4) into Fig. 10 increases the data scattering, as shown on the left side of Fig. 11, where low values of D_{ag} data reside. However, every individual data source exhibits a similar trend with respect to λ as illustrated by the linear least-square-fitting lines from the individual data sources. This is especially conspicuous from the data of Grigor'ev et al.,[7] Christian,[13] Churchill et al.,[14] and Duterque[20] shown in Fig. 8, where almost no trend can be found by Hermsen model prediction, but a better correlation with λ can be established as shown in Fig. 11. It appears that data from Murai et al.[26] exhibit a worse trend by use of the present modeling than use of Hermsen modeling. The overall correlation model for both AP/HTPB aluminized propellant and AP/nitramine/HTPB aluminized propellant by the present study is given by

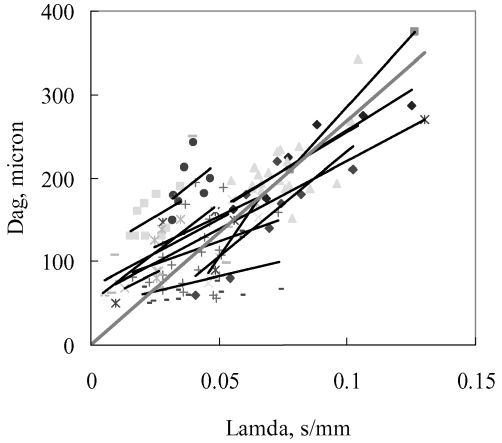

Fig. 11 Dependency of agglomerate size on lamda for aluminized composite propellants: ♦, with RDX, this work; ■, with RDX, Liu and Hsieh[2]; ▲, with HMX, Suzuki and Chiba[12]; ×, with HMX, Christian Figs. 11 and 12[13]; and ✳, with HMX, Glotov and Zarko[17,18]; ●, no nitramine, Suzuki and Chiba[12]; +, no nitramine, Christian Figs. 5–9[13]; -, no nitramine, Churchill et al.[14]; —, no nitramine, Babuk[24,25]; ♦, no nitramine, Grigor'ev et al.[7]; ■, no nitramine, Murai et al.[26]; ▲, no nitramine, Glotov and Zarko[17,18]; ×, no nitramine, Kraeutle et al.[27]; and ✳, no nitramine, Duterque.[20]

$$D_{ag} = 2694\ (\mu\text{m})\lambda \tag{7}$$

with $R^2 = 0.37$. Figure 11 shows that some data sources exhibit the segregate phenomena among themselves, especially on the left side of Fig. 11, where low values of D_{ag} data reside. This could be attributed to the bias resulting from different experimental methods, or from different definitions of agglomerate size measured, or to a limited extent from experimental conditions.

The error of using normal illumination optical method to measure agglomerate size had been the concern of previous studies,[5,7–9] and it was found that the measured size is larger than true size. However, it can be found from Fig. 11 that the data obtained by optical methods by Grigor'ev et al.,[7] Suzuki and Chiba[12] (with HMX), Duterque,[20] and the present study are almost evenly distributed along the two side of the regression model line. There is no obvious evidence that larger agglomerates are obtained by optical methods than by nonoptical methods. Only Suzuki and Chiba's[12] no-nitramine data from use of an optical method show very high values, which are accompanied by some data from nonoptical experiments. A possible explanation is that these optical experiments were conducted under rather high pressures so that the effect of oxide plume to "bloom"[5] to real diameter diminishes. Grigor'ev et al.[7] considered the pressure effect on measurement accuracy. They reported that 10–20% measurement error can occur when pressure is 40 atm.

In summary, Eq. (7) appears to give a better D_{ag} prediction than the Hermsen model prediction shown in Figs. 8 and 9 with exactly the same experimental data. Because of the very closed slope values obtained by Eqs. (6) and (7), the following equation is proposed for the prediction of D_{ag} for AP aluminized composite propellants

Table 5 Summary of Grigor'ev et al. experimental data and two model predictions

	Experimental data						Predictions			
Composition	D_{AP}, μm	P, atm (MPa)	r_{b20}, mm/s	r_{b40}, mm/s	D_{ag20}, μm	D_{ag40}, μm	Kovalev model, 20 atm	Kovalev model, 40 atm	Eq. (8), 20 atm	Eq. (8), 40 atm
2	75	40 (4.05)		8.5		60		63		104
3	110	20 (2.03)	6		80		110		147	
4	200	20 (2.03)	4.7		140		188		187	
5	280	20 (2.03)	4		180				220	
5	280	40 (4.05)		5.4		180		160		163
6	360	20 (2.03)	3.2		210		250		275	
6	360	40 (4.05)		4.5		220		200		196
7	220	20 (2.03)	4.4		170				200	

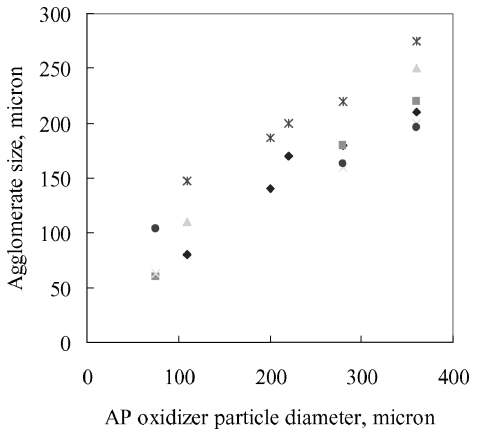

Fig. 12 Comparison of agglomerate size among Grigor'ev et al. data, Kovalev model predictions, and Eq. (8) predictions: ♦, Grigor'ev et al.[7] data, 20 atm; ■, Grigor'ev et al.[7] data, 40 atm; ▲, Kovalev[21] model prediction, 20 atm; ×, Kovalev[21] model prediction, 40 atm; ⁎, this work model prediction, 20 atm; and ●, this work model prediction, 40 atm.

containing cyclic nitramines or not:

$$D_{ag} = 2690\ (\mu\text{m})\ (\text{wt\% of Al} + \text{wt\% of cyclic nitramine} + 1)\Big/ \Big\{[\text{wt\% of AP} + \text{wt\% of cyclic nitramine}] \times r_b(\text{mm/s}) \times \left[D^0_{Al}(\mu\text{m})\Big/50 + 1\right]\Big\} \quad (8)$$

The parameter ranges, derived from Table 3 and 4, are Al wt% = 10–24, Al size = 5–50 μm, AP wt% = 27–73.2, cyclic nitramine wt% = 7.4–35, and r_b = 2.7–63 mm/s.

The validity of Eq. (8) may be tested by comparison with Kovalev's[21] recent agglomerate size prediction model. Experimental data from Grigor'ev et al.[7] and Sambamurthi et al.[10] were used to compare with Kovalev model prediction in that study.[21] Now they are also adopted here for comparison with the Eq. (8) prediction.

Table 5 lists the Grigor'ev et al. data[7] used for this comparison. Not all of experimental data reported in Ref. 7 were used. The details, as well as how the original volume fraction data are transformed to weight percentage, are denoted in footnote e of Table 4. Furthermore, due to inconsistent AP size readings between Refs. 7 and 21, AP size data from the original Ref. 7 are adopted here. Burning rate data in Table 1 of Ref. 21 are also found inconsistent with the burning rate curve. Thus, we use no data from Table 1 of Ref. 21. The burning rate data shown in Table 5 are from the burning rate curve interpolation. The predicted values from the Kovalev model are taken from Fig. 4 of Ref. 21. Calculation parameters for Eq. (8) are AP wt% = 48, Al wt% = 21, and original Al volume mean diameter = 20 μm. Figure 12 shows a comparison of agglomerate size among the Grigor'ev et al. data, Kovalev's model predictions, and Eq. (8) predictions, each under two pressures. Both the Kovalev model and Eq. (8) overpredict at under 20 atm. Both models give good predictions at under 40 atm. Furthermore, the size range predicted by the Herman model is between 218 and 579 μm for compositions 2–7.

Table 6 Summary of Sambamurthi et al. experimental data and two model predictions

Experimental data			Predictions, μm	
P, MPa	r_b, mm/s	D_{ag}, μm	Kovalev model	Eq. (8)
0.1	Unknown	160		Unknown
0.25	2.2		183	193.7
0.5	3.5	157		121.8
0.6	3.9		172	109.3
0.7	4.2	121		101.5
1	4.8		110	88.8
1.38	5.2	83		82
1.55	5.4		88	78.9
2.05	6		80	71
2.12	6.1	75		69.9

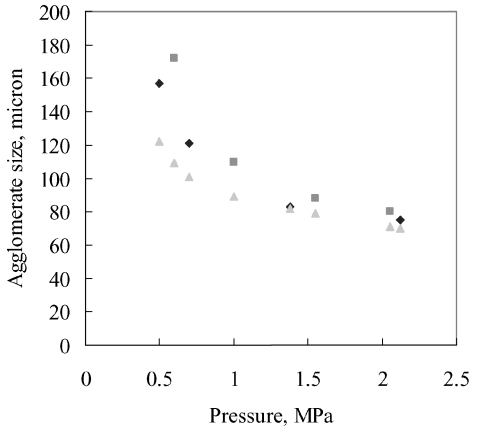

Fig. 13 A comparison of agglomerate size among ♦, Sambamurthi et al.[10] experimental data, ⊠, Kovalev[21] model predictions; and ▲, Eq. (8) predictions.

Table 6 gives the Sambamurthi et al. data[10] used for this comparison. Notice that there are no burning rate data corresponding to 0.1-MPa pressure, as shown in Fig. 7 of Ref. 21. Furthermore, burning rate under 0.25 MPa equals 2.2 mm/s, which is below the lower limit (2.7 mm/s) for the applicability of Eq. (8). Thus, we exclude these two points for comparison purposes. The calculation parameters for Eq. (8) are AP wt% = 71, Al wt% = 18, and original Al diameter = 30 μm. Figure 13 shows the comparison of agglomerate size among Sambamurthi et al. data, Kovalev's model predictions, and Eq. (8) predictions. Sambamurthi et al. data are located in a very close range between these two predictions. Furthermore, the size range predicted by the Herman model is between 205 and 569 μm for the pressure range between 2.12 and 0.25 MPa.

Conclusions

Cinephotomicrography experiments have been conducted for aluminized AP/RDX/HTPB propellant with three different virgin aluminum sizes under two different pressures. For the same aluminum size, larger agglomerates are observed under low pressures.

The contrast becomes more apparent when aluminum size becomes larger. There is an overall trend of increasing agglomerate size as virgin aluminum size decreases. However, the effect diminishes when aluminum size increases or the pressure decreases. An aluminum agglomeration mechanism based on localization of agglomeration process within propellant microstructures due to close neighboring of aluminum particles with the RDX crystal was postulated. Furthermore, Gany and Caveny's agglomeration theory indicates that the smaller value of the virgin aluminum size/mobile molten-layer thickness leads to the tendency for producing larger aluminum agglomerates. The theory can be validated from experimental data generated from three independent studies.

A new aluminum agglomerate average size prediction model based on propellant formulation and burning rate has been proposed. The model can simply explain the open literature agglomerate size data covering a wide formulation ranges and experimental conditions. The model can be useful for agglomerate size prediction of propellants containing AP as the only oxidizer, or both AP and cyclic nitramines as oxidizers. The Hermsen model, however, gives a higher prediction when compared with the same data. The validity of the new model was proven by comparison with a recent study.

Acknowledgments

The author is grateful to Min-Chio Koung, Chief Program Manager, Systems Development Center, Chung Shan Institute of Science and Technology (CSIST), for the support of the Solid Propellant Combustion Laboratory, Propellant Chemistry Section, Chemical Systems Research Division, CSIST. The author would like to thank Ing-Ming Shyu for his important contribution in the experiment. Aluminum agglomeration research results provided by O. G. Glotov, Institute of Chemical Kinetics and Combustion, Siberian Branch of Russian Academy of Sciences, through Internet communications, are acknowledged. Thanks are extended to Steve Shi-Yann Wang, founder of Solid Propellant Combustion Laboratory, CSIST, at present Research Group Leader, Pharmaceutical Research Institute, Bristol–Myers Squibb Company, New Jersey, for reviewing the manuscript and providing good suggestions. Finally, M. Brewster, Associate Editor of this journal, and anonymous reviewers are acknowledged for valuable comments and criticism of this paper.

References

[1]Liu, T. K., Perng, H. C., Luh, S. P., and Liu, F., "Aluminum Agglomeration in Ammonium Perchlorate/Cyclotrimethylene Trinitramine/Aluminum/Hydroxy-Terminated Polybutadiene Propellant Combustion," *Journal of Propulsion and Power*, Vol. 8, No. 6, 1992, pp. 1177–1184.

[2]Liu, T. K., and Hsieh, C. F., "Analysis of Agglomerate Size from Burning Aluminized AP/RDX/HTPB Propellants in Quench Bomb," *Journal of Propulsion and Power*, Vol. 12, No. 5, 1996, pp. 995–998.

[3]Luh, S. P., Liu, T. K., and Perng, H. C., "Pocket Model Application to the Combustion of AP/RDX/Al/HTPB Propellants," AIAA Paper 95-3110, July 1995.

[4]Cohen, N. S., "A Pocket Model for Aluminum Agglomeration in Composite Propellants," *AIAA Journal*, Vol. 21, No. 5, 1983, pp. 720–725.

[5]Netzer, D. W., Diloreto, V. D., and Dubrov, E., *Particle Behavior in Solid Propellant Rockets*, CPIA Publ. 329, Vol. 1, Chemical Propulsion Information Agency, Johns Hopkins Univ., Applied Physics Lab., Laurel, MD, 1980, pp. 1–19.

[6]Boggs, T. L., Crump, J. E., Kraeutle, K. J., and Zurn, D. E., "Cinephotomicrography and Scanning Electron Microscopy as Used to Study Solid Propellant Combustion," *Experimental Diagnostics in Combustion of Solids*, edited by T. L. Boggs and B. T. Zinn, Vol. 63, Progress in Astronautics and Aeronautics, AIAA, New York, 1978, pp. 20–48.

[7]Grigor'ev, V. G., Zarko, V. E., and Kutsenogii, K. P., "Experimental Investigation of the Agglomeration of Aluminum Particles in Burning Condensed Systems," *Combustion, Explosion, and Shock Waves*, Vol. 17, No. 3, 1981, pp. 245–251.

[8]Melcher, J. C., Krier, H., and Burton, R. L., "Burning Aluminum Particles Inside a Laboratory-Scale Solid Rocket Motor," *Journal of Propulsion and Power*, Vol. 18, No. 3, 2002, pp. 631–640.

[9]Melcher, J. C., IV, "Combustion of Single and Agglomerated Aluminum Particles in Solid Rocket Motor Flows," Ph.D. Dissertation Univ. of Illinois at Urbana–Champaign, IL, June 2001, pp. 87, 89, 91, 212–216.

[10]Sambamurthi, J. K., Price, E. W., and Sigman, R. K., "Aluminum Agglomeration in Solid-Propellant Combustion," *AIAA Journal*, Vol. 22, No. 8, 1984, pp. 1132–1138.

[11]Gany, A., and Caveny, L. H., "Agglomeration and Ignition Mechanism of Aluminum Particles in Solid Propellants," *Seventeenth Symposium (International) on Combustion*, Combustion Inst., Pittsburgh, PA, 1978, pp. 1453–1461.

[12]Suzuki, S., and Chiba, M., "Combustion Efficiency of Aluminized Propellant," AIAA Paper 89-2309, July 1989.

[13]Christian, T. W., "Aluminum Agglomeration in Low Burn Rate HTPB Propellants," Rept. CPTR-81-8, Chemical Propulsion Information Agency, Johns Hopkins Univ., Applied Physics Lab., Laurel, MD, Oct. 1981.

[14]Churchill, H. L., Fleming, R. W., and Cohen, N. S., "Aluminum Behavior in Solid Propellant Combustion," U.S. Air Force Rocket Propulsion Lab., CA, Rept. AFRPL-TR-74-13, May 1974.

[15]King, M. K., "Metal Combustion Efficiency Predictions for Low L* Rocket Motors," *Journal of Spacecraft*, Vol. 22, No. 5, 1985, pp. 512–513.

[16]Glotov, O. G., Zarko, V. E., and Karasev, V. V., "Problems and Prospects of Investigating the Formation and Evolution of Agglomerates by the Sampling Method," *Combustion, Explosion, and Shock Waves*, Vol. 36, No. 1, 2000, pp. 146–156.

[17]Glotov, O. G., and Zarko, V. E., "Agglomeration in Combustion of Aluminized Solid Propellants with Varied Formulation," *2nd European Conference on Launcher Technology Meeting—Space Solid Propulsion*, Rome, Nov. 21–24, 2000.

[18]Glotov, O. G., and Zarko, V. E., "Condensed Combustion Products of Aluminized Propellants," *Transactions of the Aeronautical and Astronautical Society of the Republic of China*, Vol. 35, No. 3, 2003, pp. 247–260.

[19]Hermsen, R. W., "Aluminum Combustion Efficiency in Solid Rocket Motors," AIAA Paper 81-0038, Jan. 1981.

[20]Duterque, J., "Experimental Studies of Aluminum Agglomeration in Solid Rocket Motors," *4th International Symposium on Special Topics in Chemical Propulsion* ONERA TP 1996-48, http://www.onera.fr/RECH/BASIS/public/web_fr/document/DDD/243366.pdf [cited 12 April 2004].

[21]Kovalev, O. B., "Motor and Plume Particle Size Prediction in Solid-Propellant Rocket Motors," *Journal of Propulsion and Power*, Vol. 18, No. 6, 2002, pp. 1199–1210.

[22]Price, E. W., "Combustion of Metalized Propellants," *Fundamentals of Solid-Propellant Combustion*, edited by K. K. Kuo and M. Summerfield, Vol. 90, Progress in Astronautics and Aeronautics, AIAA, New York, 1984, Chap. 6, pp. 479–513.

[23]Price, E. W., and Sigman, R. K., "Combustion of Aluminized Solid Propellants," *Solid Propellant Chemistry, Combustion, and Motor Interior Ballistics*, edited by V. Yang, T. B. Brill, and W. Z. Ren, Progress in Astronautics and Aeronautics, Vol. 185, AIAA, Reston, VA, 2000, pp. 663–687.

[24]Babuk, V. A., "Study of Metal Agglomeration and Combustion," Final Rept. Contract F61708-96-W0269, Baltic State Technical Univ., St. Petersburg, Russia, 27 Dec. 1996.

[25]Babuk, V. A., Vasilyev, V. A., and Malakhov, M. S., "Condensed Combustion Products at the Burning Surface of Aluminized Solid Propellant," *Journal of Propulsion and Power*, Vol. 15, No. 6, 1999, pp. 783–793.

[26]Murai, H., Kobayashi, N., Hori, K., and Kohno, M., "Suppressive Effect Prediction of Aluminum Particles on SRM Longitudinal Acoustic Oscillation (in Japanese)," *Proceedings of Symposium on Space Transportation*, Inst. of Space and Astronautical Science, Dec. 1992.

[27]Kraeutle, K. J., Reed, R., Jr., Atwood, A. I., and Mathes, H. B., "Effect of Binder Type on Aluminum Combustion and Aluminum Oxide Formation," *16th JANNAF Combustion Meeting*, CPIA Publ. 308, Vol. 2, Chemical Propulsion Information Agency, Johns Hopkins Univ., Applied Physics Lab., Laurel, MD, 1979, pp. 225–236.

[28]Kohno, M., Saito, T., Tokudome, S., Volpi, A., Kato, K., Kimura, M. Maruizumi, H., and Hirai, K., "Subatmospheric Combustion of Aluminized Composite Propellants and SRM Residual Chamber Pressure," *Proceedings of the 19th International Symposium on Space Technology and Science*, Paper No. ISTS-94-a-33, Yokohama, 1994, pp. 117–128.